В-69
2735/2-76

ОБЪЕДИНЕННЫЙ
ИНСТИТУТ
ЯДЕРНЫХ
ИССЛЕДОВАНИЙ
ДУБНА

19/VII-76

E7 - 9626

B.Bochev, S.A.Karamian, T.Kutsarova, E.Nadjakov,
Yu.Ts.Oganessian

THE FEEDING TIMES AND LIFETIMES OF HIGH-SPIN LEVELS IN YTTERBIUM DOUBLY EVEN ISOTOPES

1976

E7 - 9626

B.Bochev, S.A.Karamian, T.Kutsarova, E.Nadjakov,
Yu.Ts.Oganessian

THE FEEDING TIMES AND LIFETIMES OF HIGH-SPIN LEVELS IN YTTERBIUM DOUBLY EVEN ISOTOPES

Submitted to "Nuclear Physics"

1. INTRODUCTION

High-spin nuclear states have recently been investigated in detail using γ-ray spectroscopic methods on α-particle and heavy ion beams. In particular, the spectra of prompt γ-rays emitted from excited nuclei formed in reactions on target nuclei have been measured. This method has a number of advantages compared with techniques based on the spectroscopy of radioactive sources.

The study of high-spin nuclear states has several aspects.

First, the energy position of nuclear levels as a function of spin for the g.s.b. and β- and γ-bands is of great theoretical interest that is growing after the discovery of "backbending" in 1971 (see refs. /1-4/ for experimental and theoretical reviews) and of related phenomena such as "downbending" at still higher spins /1,5,6/ , and the intersection of the ground-state and β-bands ("double backbending" /7,8/). The γ-spectroscopy experiments carried out on beams during the recent years have provided a large amount of new information about the level scheme of neutron-deficient isotopes, which were difficult to investigate using the radioactive

source spectroscopy. It is also important that these experiments enabled one to follow up the rotational bands of many deformed nuclei up to levels with spins of (20-22) $\hbar$. From the level energy of the rotational band, it is easy to deduce the moment of inertia $J = 3/E_2$ of the nucleus in the ground state and the dependence of the moment of inertia on spin $J(I)$. The unexpected features of this function (i.e., $J(\hbar^2\omega^2)$, where ω is the frequency of nuclear rotation) have been termed "backbending", "downbending" and "double backbending".

Second, measurements of the lifetimes of rotational levels permit determination of the reduced probabilities of electromagnetic transitions $B(E2, I \longrightarrow I-2)$ as well as the quadrupole moment $Q(I)$ and deformation parameter $\beta(I)$ as a function of spin (see, e.g., formulae in ref./9/). The recoil-distance Doppler-shift method /10/ was used in several laboratories to measure the lifetimes of rotational levels of deformed rare-earth nuclei produced in compound-nucleus reactions with neutron emission, (HI, xn), induced by heavy ions /9, 11 - 13/. This method has recently been extended to the region of high-spin states, where the backbending effect takes place /14, 15/. The experimental values of $B(E2, I \longrightarrow I-2)$ for transitions in the backbending zone, normalized to $B_{rot}(E2, I \longrightarrow I-2)$ of the rigid rotor, can clarify the nature of backbending if a fairly good experimental accuracy is achieved. We are aware of different proposals as to how to interpret its mechanism. They are:
1) The Coriolis antipairing predicted many

years ago [16] (see ref. [17] for one of its treatments and for the literature); 2) Rotation alignment or the decoupling of a pair of particles [18]; and 3) Changes in deformation [19, 20] or, to be more exact, in the form of potential energy vs. deformation with increasing spin, and, possibly, the appearance of instability with respect to non-axial deformations [21].

Third, the mechanism of the population of rotational bands (refs. [22,23]) is of great interest in view of small amounts of both theoretical and experimental data on the cascades of transitions which take place during the decay of the initial highly-excited high-spin compound nucleus to the states of bands observed in the experiment. During the recent few years, measurements were carried out of the multiplicity of γ-rays during the population of yrast bands in the cascades of statistical γ-radiation following compound nucleus reactions involving neutron evaporation [24-26]. Simultaneously with the measurements of rotational states lifetimes, some data were obtained concerning the feeding times of individual levels [11,14,15,27] and the intensity of level population as a function of spin. These results provided the systematics of mean square momenta of the levels populated, $\sqrt{\langle I^2 \rangle}$, and permitted some conclusions about the main features of the cascades leading to the level population [28].

2. EXPERIMENTAL

As is known, the recoil-distance Doppler-shift method consists in measuring the energy

and intensity of the γ-rays of electromagnetic transitions in recoil nuclei following (HI, xn) reactions provided that the nuclei recoiling from the target pass some distance d in vacuum to be stopped in the plunger. The distance d between the target and the plunger should be varied over a wide range and fixed with a high accuracy for each measurement.

The experimental arrangement used was the same as that described previously /29/, the only difference being the use of a new high-precision Doppler chamber (Fig. 1). The distance between the target and plunger was measured with an $1\mu m$ accuracy; this implied an error of 20% for a time-of-flight of about 1 ps. The accuracy of parallelism between the operating surface of the target and the plunger, and of the setting of the zero distance was no worse than $2\mu m$. The zero distance was measured using the method of capacity measurements /30/.

The levels of Yb nuclei were populated in the reactions $^{124-130}_{52}Te(^{40}_{18}Ar, 4n)^{160-166}_{70}Yb$. In the experiments, an external heavy ion beam from the Dubna U-300 cyclotron was used. The beam diameter was limited by a collimator consisting of three Bi diaphragms. Metallic targets, 1 mg/cm^2 thick, were prepared by evaporating separated Te isotopes onto a $0.7\mu m$ Al backing stretched on a Bi lattice. Recoil nuclei were stopped in a Bi covered plunger. The use of bismuth in all parts of the experimental set-up which are exposed to the beam was necessitated by the intensity of background γ-radiation to be reduced compared with the flux of γ-rays arising from nuclear reactions on the target substance. A detector

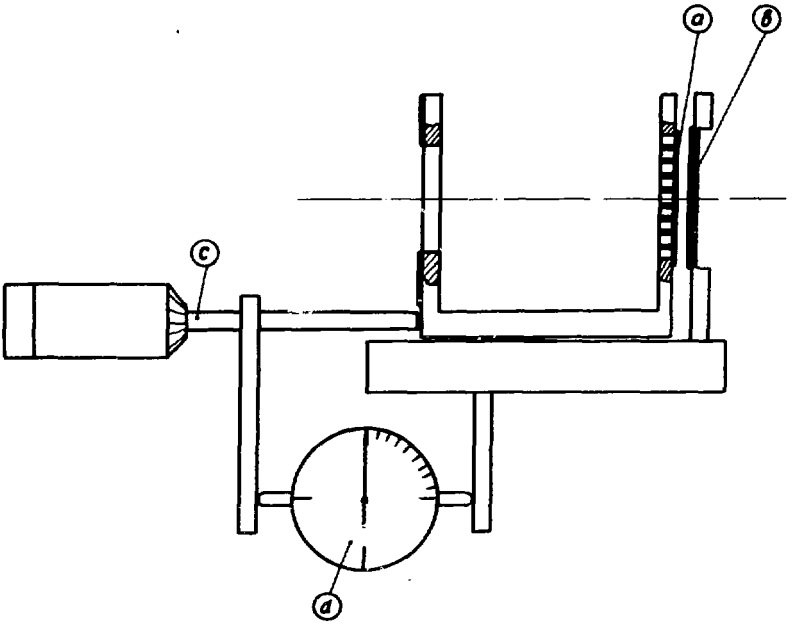

Fig. 1. Doppler chamber: (a) target with a system for zero-distance adjustment; (b) plunger with a system for making it parallel to the target; (c) micrometer screw moving the target; (d) high-precision indicator measuring the target-to-plunger distance.

with an active volume of 34 cm^3 and resolution of 2.4 keV was used for most transitions, while for low energy transitions ($E_\gamma < 200$ keV) a detector with a volume of 1 cm^3 and resolution of 1.2 keV at 122 keV was employed. These resolutions were sufficient to separate the Doppler-shifted peak from the unshifted one at recoil velocities of about $v/c \sim 0.02$. Use was also made of a switching scheme which sent the working spectrum during cyclotron pulses and the background spectrum between the pulses to different multichannel analyzers. This eliminated long-lived back-ground activities with a lifetime of $\tau \geq 1$ ms from the working spectrum. The background spectrum was recorded in the second analyzer to provide information about the energy and intensity of background peaks.

The experiment was carried out repeatedly at different distances between the target and plunger, corresponding to different times-of-flight $t = d/v$ of recoil nuclei. To detect and extract short-lived background peaks, the experiment was also performed at a "zero" and "infinite" distance between the target and plunger. At any distance, for each transition the spectrum shows two peaks (refs./9,11/), i.e., an unshifted peak (u) with the correct energy E_u and intensity N_u, which is due to nuclei stopped in the plunger, and a Doppler shifted peak (s) at an energy $E_s = (1+v/c)E_u$ with intensity N_s, which is associated with nuclei emitting γ-rays in flight. From the measured E_u and E_s, after making corrections for a finite counter solid angle one can determine v and thereby

t . From the measured N_u and N_s it is possible to determine the relative intensities $R_I = N_u/(N_u + N_s)_{I \longrightarrow I-2}$, which decrease like linear combinations of exponentials[9,12] as a function of the time-of-flight t (Figs.2 and 3 and eq. (3) of the following section). The functions $R_I(t)$ are experimentally obtained decay curves of levels I .

3. DATA HANDLING

The lines of transitions between rotational states were sought for in spectra at energies determined in the literature. We obtained energies by a least-square fit to those from refs.[1,2,31]. The intensities N_u and N_s were found from the peak areas after the subtraction of the background peaks with corrections for detector efficiency and internal conversion. To eliminate background peaks, the working spectra were decomposed using the information obtained from the background spectra and from the working spectra at the "zero" and "infinite" distance. In the cases of overlapping background peaks their intensities were determined from the spectra at the "zero" and "infinite" distances and subtracted from N_s and N_u, respectively.

Thus, the integral, $N_I = (N_u + N_s)_{I \longrightarrow I-2}$, and differential $P_I = N_I - N_{I+2}$, intensities were obtained (Fig. 4). The $P_I / \Sigma P_I$ ratio represents the relative intensity of the sidefeeding of level I . The I dependence of N_I was used to restore the intensity N_u or N_s of the peak superimposed on a very high (e.g. annihilation) background peak by interpolating N_I to adjacent transitions.

Fig. 2. Decay curves of relative intensities $R_I (I \geq 6)$ versus time-of-flight t for ^{164}Yb. . Points are experimental results for the following transitions: 6 → 4 (O) ; 8 → 6 (□); 10 → 8 (x); 12 → 10 (O); 14 → 12 (+); 16 → 14 (Δ); 18 → 16 (x). Solid lines are the calculated best fit curves.

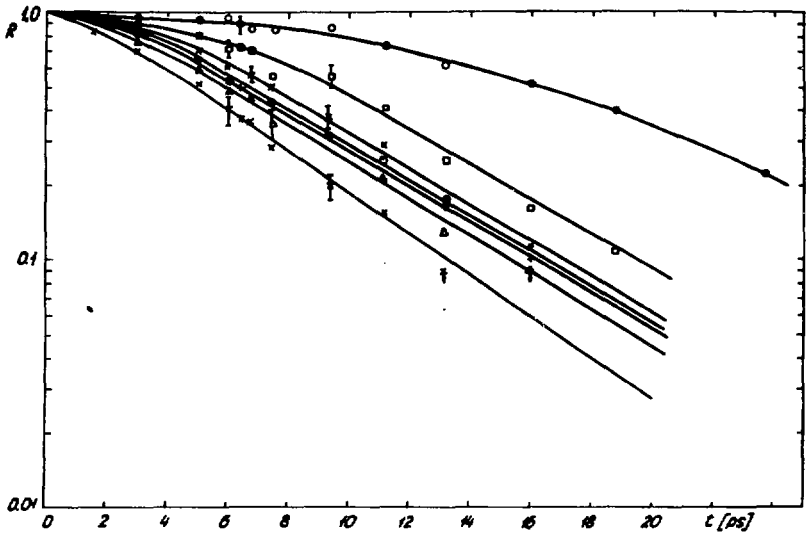

Fig. 3. Decay curves of relative intensities R_I versus time-of-flight t for ^{166}Yb: a) for transitions 2 → 0 (□); 4 → 2 (x) and 6 → 4 (O); , and b) for transitions 6 → 4 (O); 8 → 6 (□); 10 → 8 (x); 12→10 (O); 14→ 12(+); 16 → 14 (Δ); 18 → 16(x); 20→ 18(□) .Solid lines are the calculated best fit curves.

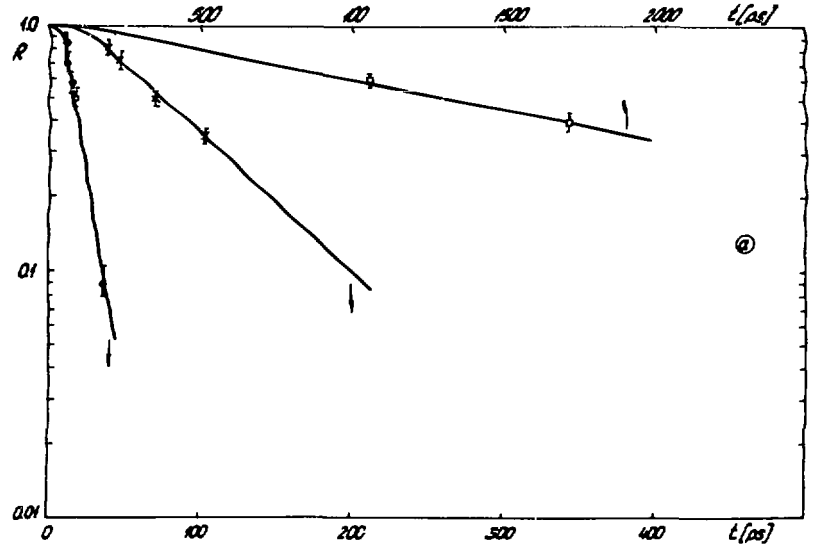
1.0
R
0.1
0.01
0
100
200
300
400
t[ps]
500
600
1500
2000
t[ps]
а

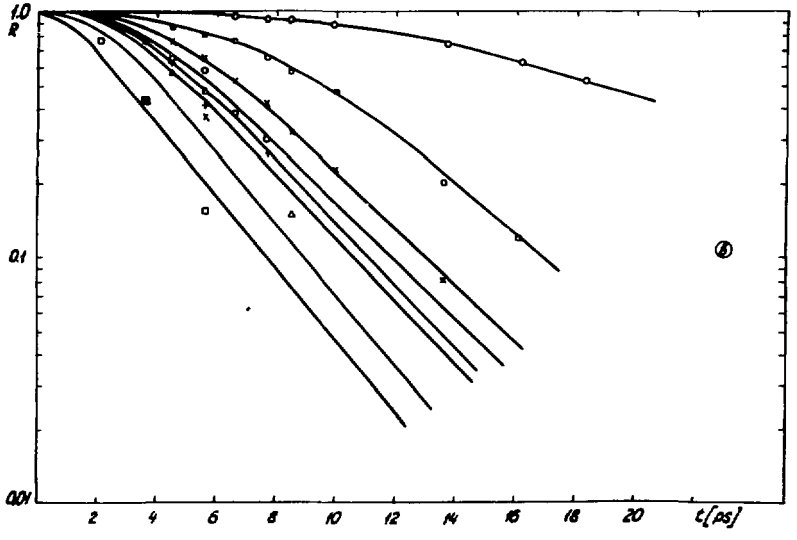
1.0
R
0.1
0.01
2
4
6
8
10
12
14
16
18
20
t[ps]
б

As many as seven corrections /32,12/ were introduced using a standartized procedure in order to obtain from $N_u/(N_u + N_s)$ the corrected quantities of $R_I = R_I(t)$ together with their statistical inaccuracies. Four of the corrections were usually negligible under our conditions. The correction for attenuation in the anisotropy of the γ-ray angular distribution /32, 33/ was not negligible. At large distances, the most important correction (which was substantial only for $2 \longrightarrow 0$ transitions) was due to changes in the counter solid angle /16/. At small distances, it was the correction due to the finite range of recoil nuclei in the plunger (important for all transitions from $6 \longrightarrow 4$ upwards at times-of-flight below 10 ps) /16/. This correction was modified here by taking into account very short lifetimes (1-2 ps) of transitions in the backbending region in the following way

$$R_{corr}(t_{corr}) = [e^{x\Delta t/\tau} + e^{-t/\tau} - e^{-(t-2x\Delta t)/\tau}] R_{uncorr}(t_{uncorr}), \quad (1)$$

where τ is the mean lifetime of the transition if its decay curve $R(t)$ is approximated by one exponential $e^{-t/\tau}$; $\Delta t = \Delta d/v$, where Δd is the range of recoil nuclei in the plunger (usually $\Delta t \sim 1$ ps); $x = (E_s - E_u - \Delta E)/(E_s - E_u)$ (ΔE is the peak width, x being usually equal to about 0.5); $t = t_{corr} = t_{uncorr} + \Delta t$.

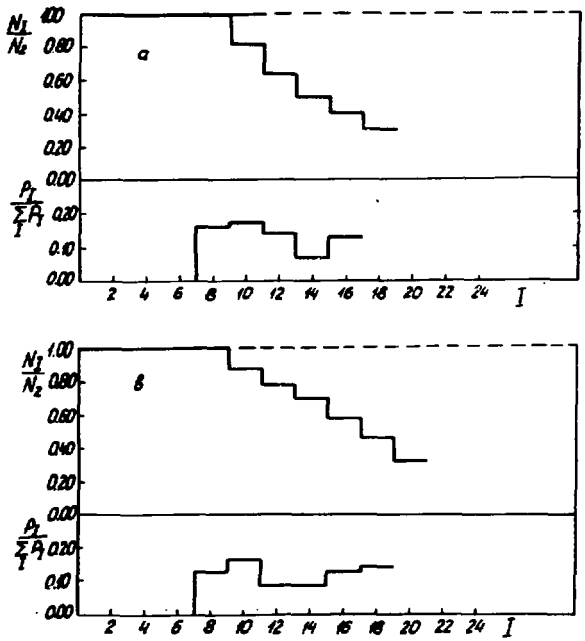

Fig. 4. Relative integral N_I / N_2 intensity of feeding and relative differential $P_I / \sum_I P_I$ intensity of side feeding as a function of spin I for the following reactions:
a) $^{128}Te(^{40}Ar, 4n)^{164}Yb$, $^{130}Te(^{40}Ar, 4n)^{166}Yb$.

The last stage is the determination of the mean lifetimes τ_I and side feeding time ϕ_I of level I. For this purpose we can consider the feeding of level I and thus the theoretical value of $R_I(t)$ as a superposition of chain transitions starting from levels K(K = I_m, $I_m - 2$, ... I, , where I_m is the highest level) with a side feeding time ϕ_k and lifetimes τ_k. Each of these chains contributes to a ratio $R_I(t)$ (given in [9,12]) with a weigth $P_k / \sum_{k'=I}^{I_m} P_{k'}$.

$$R_I(t) = \sum_{k=I}^{I_m} P_k / \left(\sum_{k'=I}^{I_m} P_{k'} \right) \cdot R_I^k(t). \qquad (2)$$

This expression, together with formulae from refs. [9, 12], , gives

$$R_I(t) = \sum_{M=k}^{I_m} \left(A_I^k e^{-t/\tau_k} + B_I^k e^{-t/\phi_k} \right), \qquad (3)$$

where

$$A_I^k = \sum_{M=k}^{I_m} P_m / \left(\sum_{k'=I}^{I_m} P_{k'} \right) \cdot \frac{\tau_k}{\tau_k - \phi_M} \prod_{L=I (L \neq k)}^{M} \frac{\tau_k}{\tau_k - \tau_L},$$

$$B_I^k = P_k / \left(\sum_{k'=I}^{I_m} P_{k'} \right) \cdot \prod_{L=I}^{k} \frac{\tau_k}{\phi_k - \tau_L}. \qquad (4)$$

The τ_I and ϕ_I values were determined by a fit of eq. (3) to the experimental value of $R_I(t)$ using regularized iterative processes of the Gauss-Newton type /34/ or a least square fit at a computer. Figures 2 and 3 show a comparison of theoretical fits (solid line) with experimental points for two cases.

One should note that the experiment allows a certain freedom in the correlated choice of τ_I and ϕ_I in the sense that an increase in ϕ_I can to some extent compensate for a decrease in τ_I or vice versa. This concerns high-spin levels where side feeding is not negligible compared with the total feeding intensity. To check this point, a series of calculations have been carried out at fixed τ_I or ϕ_I ranging from zero to very high values. This analysis has shown that the automatically computed values of τ_I and ϕ_I and their errors are reliable.

4. RESULTS

The results on E_I, P_I, ϕ_I and τ_I for all ytterbium isotopes investigated are shown in Table 1. For comparison, the rigid rotor values of τ_I deduced from the experimental value of τ_2 and from the rigid rotor reduced transition probabilities $B_{rot}(E2; I \to I-2)$ are also given. The results of Table 1 are an extension of our previous work /13, 35-37/.

It is noteworthy that P_{I_m} for the highest level I_m is equal to N_{I_m} since one cannot separate its side feeding P_{I_m} from its total feeding N_{I_m}. Also, ϕ_{I_m} is a composite quantity representing an average total feeding

Table 1

Transition energies $E_{I \to I-2}$, relative side feeding intensities $P_I / \sum_I P_{I'}$, mean side feeding times ϕ_I and lifetimes τ_I (at spin I) of the yrast bands of ^{166,164,162,160}Yb

Nucleus	Level I	$E_{I \to I-2}$ [keV] Ref.[23]	This work	$P_I / \sum_I P_I$	ϕ_I [ps]	τ_I [ps] Experiment	Rigid rotor
$^{160}_{70}Yb_{90}$	2	243.0	243.1	0	—	182 ± 6	182 a)
	4	395.3	395.4	0	—	11.6 ± 0.60	12.38
	6	508.8	508.8	0	—	2.73 ± 0.30	3.235
	8	588.7	588.7	0	—	1.29 ± 0.30	1.498
	10	(636)	636	1	12.5 ± 2	0.87 ± 0.50	0.993
$^{162}_{70}Yb_{92}$	2	166.5	166.5	0	—	578 ±65	578 a)
	4	320.2	320.3	0	—	20.3 ± 3.0	21.71
	6	436.2	436.2	0	—	4.6 ± 0.9	4.352
	8	521.4	521.4	1	10 ± 3	2.0 ± 0.7	1.720
$^{164}_{70}Yb_{94}$	2	123.3	123.5	0	—	1272 ±50	1272 a)
	4	262.4	262.8	0	—	42.8 ± 1.5	44.54
	6	374.7	375.0	0	—	7.24 ± 0.25	7.298
	8	463.0	463.0	0.16 ± 0.01	6.3 ± 5.3	2.20 ± 0.70	2.472
	10	530.9	530.9	0.17 ± 0.01	5.1 ± 4.2	1.19 ± 0.40	1.222
	12	576.9	576.9	0.14 ± 0.01	4.8 ± 3.2	0.80 ± 0.30	0.794
	14	569.7	569.7	0.06 ± 0.01	2.3 ± 1.1	1.05 ± 0.30	0.836
	16	490.0	490	0.12 ± 0.015	1.3 ± 0.5	2.53 ± 0.50	1.748
	18	543.2	543	0.35 ± 0.035	5.3 ± 1.5	1.07 ± 0.50	1.042
$^{166}_{70}Yb_{96}$	2	102.26	102.3	0	—	1789 ±90	1789 a)
	4	228.05	227.9	0	—	76.3 ± 2.5	75.10
	6	337.3	337.7	0	—	11.24 ± 0.40	10.64
	8	430.4	430.2	0.13 ± 0.02	3.8 ± 1.8	3.09 ± 0.35	3.109
	10	507.5	~ 507.3	0.16 ± 0.04	3.7 ± 3.1	1.46 ± 0.70	1.339
	12	569.3	569.8	0.09 ± 0.03	2.5 ± 2.2	0.93 ± 0.47	0.737
	14	603.3	603.5	0.09 ± 0.03	3.0 ± 2.2	0.73 ± 0.42	0.547
	16	494.5	494.1	0.13 ± 0.03	3.0 ± 1.5	1.65 ± 0.39	1.467
	18	509.1	~ 509.2	0.14 ± 0.04	2.0 ± 2.3	—	1.253
	20	588.8	588.4	0.26 ± 0.05	2.8 ± 2.1	—	0.608

*Normalized to experiment.

time including side feeding and feeding via to the band.

5. PROPERTIES OF ROTATIONAL STATES

From the 2^+ level lifetimes (Table 1) one can easily deduce the $B(E2, 2 \to 0)$ values, intrinsic electric quadrupole moments $Q(2 \to 0) = Q$ and quadrupole deformation parameters $\beta(2 \to 0) = \beta$. These parameters, together with the energy ones, moment of inertia $J = 3/E_{2 \to 0}$ and energy ratio E_4/E_2, are given in Table 2. One can see that all parameters decrease with decreasing A, i.e., as N approaches the magic number 82. In our case of Z =70, the nucleus with A =162 and N = 92 (i.e., 10 neutrons above the magic number 82) can be considered as the beginning of the transitional region where deformed nuclei become spherical.

Table 3 presents the values of $B(E2; I \to I-2)$, $Q(I \to I-2)$ and $\beta(I \to I-2)$ deduced from the experimental values of τ_I (Table 1) using formulae [9]. The values of $B(E2; I \to I-2)$ calculated in the framework of the rigid rotor model and normalized to the experimental values of $B(E2; 2 \to 0)$ are also given for comparison. Neither Q nor β parameter depends on spin in the rigid rotor model.

In the case of $^{160}_{70}Yb$, , the softest transitional nucleus of those investigated, one observes the tendency of increasing $B(E2)/B_{rot}(E2)$, Q , and β with the spin in agreement with the centrifugal stretching model. Such an effect was also observed for the nuclei of $^{156}_{68}Er$, $^{158}_{68}Er$ (refs. [11, 14]) and for the isotopes $_{62}Sm$,

Table 2

Moments of inertia $J = 3/E_{2\to 0}$, energy ratios $E_4/E_2 = (E_{4\to 2}+E_{2\to 0})/E_{2\to 0}$, intrinsic E2-moments $Q = Q(2\to 0)$ and quadrupole deformation parameters $\beta = \beta(2\to 0)$ of the Yb isotopes

Nucleus	$\mathcal{J}$ [MeV^{-1}]	E_4/E_2	Q [barn]	β
$^{160}_{70}Yb_{90}$	12.34	2.626	4.81 ± 0.08	0.207 ± 0.003
$^{162}_{70}Yb_{92}$	18.02	2.924	6.07 ± 0.45	0.257 ± 0.019
$^{164}_{70}Yb_{94}$	24.29	3.128	6.79 ± 0.13	0.284 ± 0.006
$^{166}_{70}Yb_{96}$	29.33	3.228	7.26 ± 0.18	0.301 ± 0.008

and $_{64}Gd$ (refs. [38, 39]). As a rule, the extent of $B(E2)/B_{rot}(E2)$ variations with spin is characterized by a mixing or stretching parameter α [38, 39]. In our case of $^{160}_{70}Yb$, , $\alpha = (2 \pm 1) \times 10^{-3}$. The microscopic theory [40-43] gives close values. In all other isotopes of $^{162-166}_{70}Yb$ with more stable deformation, changes in E2 moments remain within experimental errors; the upper limit for these isotopes being $\alpha \leq 0.5 \times 10^{-3}$ which agrees with the predictions of the theoretical papers cited.

The behaviour of $B(E2; I \to I-2)$ in the vicinity of the backbending region is of special interest. The data of Table 3 show that for transitions $14 \to 12$ and $16 \to 14$ in $^{164}_{70}Yb$, , and $10 \to 8$ to $16 \to 14$ in $^{166}_{70}Yb$ one observes the tendency of retarded transitions compared with the rigid rotor model. The same picture was observed in the cases of $^{158}_{68}Er$ (ref [14]) and $^{130}_{58}Ce$ (ref. [15]). All of the known factors $B(E2)/B_{rot}(E2)$ for transitions in the backbending region are listed in Table 4.

These experimental results show that one should consider only such models of the backbending phenomenon, which give a drastic increase in the moment of inertia J with spin I, but only small changes (a decrease) in the intrinsic E2 moment Q. Thus one can eliminate effects due to strong changes in deformation. This confirms the point of view of some authors [44] that they play an inconsiderable role for well deformed nuclei. On the other hand, the experiment is in good agreement with models involving some changes in pairing since, as is well known, they influence J strongly [45] and almost do not change Q (ref. [46]). So the Coriolis antipair-

Table 3

Reduced transition probabilities B(E2), enhancement $B(E2; I \to I-2)/B_{rot}(E2; I \to I-2)$ factors, intrinsic E2-moments $Q(I \to I-2)$ and deformations $\beta(I \to I-2)$ up the yrast bands in the Yb isotopes

Nucleus	Transition I→I-2	B(E2,I→I-2) Experiment	$[e^2 b^2]$ Rigid rotor	$\frac{B(E2,I \to I-2)}{B_{rot}(E2,I \to I-2)}$	Q(I→I-2) [barn]	β
$^{160}_{70}Yb_{90}$	2→0	0.460 ± 0.015	0.460 a)	1.000 ± 0.033	4.81 ± 0.08	0.207 ± 0.003
	4→2	0.701 ± 0.036	0.657	1.067 ± 0.055	4.97 ± 0.13	0.214 ± 0.006
	6→4	0.858 ± 0.094	0.724	1.185 ± 0.130	5.24 ± 0.29	0.225 ± 0.012
	8→6	0.88 ± 0.20	0.758	1.16 ± 0.27	5.18 ± 0.60	0.223 ± 0.026
	10→8	0.89 ± 0.51	0.778	1.14 ± 0.65	5.14 ± 1.48	0.221 ± 0.064
$^{162}_{70}Yb_{92}$	2→0	0.732 ± 0.108	0.732 a)	1.000 ± 0.147	6.07 ± 0.45	0.257 ± 0.019
	4→2	1.119 ± 0.165	1.046	1.070 ± 0.158	6.28 ± 0.46	0.266 ± 0.020
	6→4	1.09 ± 0.21	1.152	0.95 ± 0.18	5.90 ± 0.58	0.250 ± 0.024
	8→6	1.04 ± 0.36	1.206	0.86 ± 0.30	5.63 ± 0.98	0.239 ± 0.042
$^{164}_{70}Yb_{94}$	2→0	0.918 ± 0.036	0.918 a)	1.000 ± 0.039	6.79 ± 0.13	0.284 ± 0.005
	4→2	1.364 ± 0.048	1.311	1.040 ± 0.037	6.93 ± 0.12	0.290 ± 0.005
	6→4	1.456 ± 0.050	1.444	1.008 ± 0.035	6.82 ± 0.12	0.285 ± 0.005
	8→6	1.70 ± 0.54	1.512	1.124 ± 0.172	7.20 ± 1.15	0.301 ± 0.048
	10→8	1.59 ± 0.54	1.553	1.03 ± 0.34	6.88 ± 1.16	0.288 ± 0.048
	12→10	1.57 ± 0.59	1.581	0.99 ± 0.37	6.77 ± 1.27	0.283 ± 0.053
	14→12	1.27 ± 0.36	1.600	0.80 ± 0.23	6.06 ± 0.87	0.255 ± 0.036
	16→14	1.12 ± 0.22	1.615	0.69 ± 0.14	5.65 ± 0.56	0.238 ± 0.024
	18→16	1.59 ± 0.74	1.629	0.97 ± 0.45	6.71 ± 1.57	0.281 ± 0.066
$^{166}_{70}Yb_{96}$	2→0	1.050 ± 0.053	1.050 a)	1.000 ± 0.050	7.26 ± 0.18	0.301 ± 0.008
	4→2	1.473 ± 0.048	1.500	0.982 ± 0.032	7.20 ± 0.12	0.298 ± 0.005
	6→4	1.564 ± 0.056	1.652	0.947 ± 0.034	7.07 ± 0.13	0.293 ± 0.005
	8→6	1.739 ± 0.197	1.729	1.006 ± 0.114	7.29 ± 0.41	0.302 ± 0.017
	10→8	1.63 ± 0.78	1.776	0.92 ± 0.44	6.96 ± 1.67	0.289 ± 0.069
	12→10	1.44 ± 0.72	1.808	0.80 ± 0.40	6.48 ± 1.63	0.269 ± 0.068
	14→12	1.38 ± 0.79	1.830	0.75 ± 0.43	6.30 ± 1.81	0.262 ± 0.075
	16→14	1.64 ± 0.39	1.848	0.89 ± 0.21	6.85 ± 0.81	0.284 ± 0.034

*Normalized to experiment

ing effect should give relative retardation of transitions by a factor of 1.1-1.25 (refs. /3, 44, 47/) and rotation alignment by a factor of no more than 1.1 (ref. /18/). Both of these values agree with experiment.

6. FEEDING OF HIGH-SPIN STATES

The data presented in Table 1 and Fig. 4 show that the active side feeding represented by its relative intensity $P_I / \Sigma P_I$ is close to 0 for low spins, starts at about I = 8, , remain nearly constant over a large range of spin values and ends at I =20-24. This makes it impossible to observe the higher spin levels of the band. From these data one can calculate the mean square angular momentum $\sqrt{<I^2>}$ of the level populated, which turns out to be equal to 17.5 and 16.5 for $^{164}_{70}$Yb and $^{166}_{70}$Yb, , respectively. One can notice immediately that these values are about a factor of 3 smaller than the mean square angular momentum $\sqrt{<\ell^2>}$ of the compound nucleus, which was calculated in the framework of the model of a black nucleus. On the other hand, they coincide fairly well with the backbending point. This enables one to put forward the following hypothesis.

In the vicinity of $\sqrt{<I^2>}$, the yrast band is connected with higher-lying high-spin levels by transitions with enhanced probability. This is in agreement with the well-known model of band hybridization for the interpretation of backbending /48/. This model suggests an enhanced probability for transitions to the yrast line in the vicinity of the intersection of bands.

Table 4

Enhacement $B(E2)/B_{rot}(E2)$ factors of transitions in the back bending region

Transition $I \rightarrow I-2$ \ Nucleus	$B(E2; I \rightarrow I-2)/B_{rot}(E2; I \rightarrow I-2)$			
	$^{130}_{58}Ce$ /15/	$^{158}_{68}Er$ /14/	$^{164}_{70}Yb$	$^{166}_{70}Yb$
$12 \rightarrow 10$	0.75 ± 0.19	≥ 1	0.99 ± 0.37	0.77 ± 0.28 *)
$14 \rightarrow 12$	—	0.80 ± 0.19	0.80 ± 0.23	
$16 \rightarrow 14$	—	1.4 ± 0.35	0.69 ± 0.14	0.89 ± 0.21
$18 \rightarrow 16$	—	> 0.6	0.97 ± 0.45	—

*Both transitions have been unified to obtain better accuracy (separate values see in Table 3).

Table 5

Feeding times θ_I

Level I / Reaction	θ_I [ps] 20	18	16	14	12	10	8	6
$^{115}In(^{19}F,4n)^{130/120/}Ce$				3	9	10	12	
$^{130}Te(^{32}S,4n)^{158/159/}Er$		2.2	4.8	6	7.5	8.6	10	14
$^{124}Te(^{40}Ar,4n)^{160}Yb$						13 ±1.5	14 ±2	17 ±2
$^{126}Te(^{40}Ar,4n)^{162}Yb$							12 ±3	16 ±4
$^{128}Te(^{40}Ar,4n)^{164}Yb$		6.5±1.5	8.0 ±1.5	8.3±1.5	8.7 ±1.5	9.4 ±2	11.8±2	19.7±2
$^{130}Te(^{40}Ar,4n)^{166}Yb$	3.7 ±2	4.9±2.5	6.2 ±1.5	6.6±1.5	7.2±1.5	8.3 ±2.5	11.2±2	20.9±2

In ref. [28], the situation with $\sqrt{\langle I^2\rangle}/\langle \ell^2\rangle$ observed here was shown to be a common feature of the reactions. This ratio decreases regularly with increasing projectile mass. In addition to the hypothesis mentioned above, in ref. [28] other two hypotheses are considered for the explanation of the small value of $\sqrt{\langle I^2\rangle}$. These are: 1. The critical angular momentum of the compound nucleus is in fact close to $25\hbar$, i.e., substantially smaller than that calculated in the framework of the black nucleus model; 2. The distribution over the angular momentum of fixed final products of neutron evaporation is characterized by an average angular momentum considerably smaller than $\sqrt{\langle \ell^2\rangle}$. Both of these hypotheses were rejected after an appropriate analysis [28].

In addition to feeding intensities, Table 1 presents also the side feeding times ϕ_I. The values of ϕ_I should be distinguished from the commonly used feeding times θ_I (refs. [11, 27]), an average interval of time between the end of the reaction and the decay of the highest-lying high-spin level I_m observed. The θ_I value is clearly seen to be a composite quantity dependent on both the lifetimes $\tau_{I'}$ and feeding times $\phi_{I'}$ of all levels $I' \geq I$, through which the feeding of the observed level I occurs. The θ_I values are deduced from the experiment more easily than the ϕ_I ones. Some data on the feeding times θ_I for the isotopes $_{70}Yb$, $^{158}_{68}Er$, $^{130}_{58}Ce$ investigated [14, 15] are presented in Table 5. The θ_I value is seen to increase substantially with decreasing spin I. In addition, one can notice that at constant I θ_I tends

to increase with decreasing N, i.e., as one goes to the softer nuclei. This was also indicated previously [11,27]. However, this change in θ_I is noticeable only for high spins and becomes weaker as one moves downwards along the band. It may be more appropriate to compare the θ_I values at close energies of the rotational levels, E_I, rather than at the same spin. In this case the tendency of θ_I to increase would become more pronounced for nuclei of the transitional region. Nevertheless, for all nuclei the θ_I values are of the order of several picoseconds for the upper levels of the yrast band.

As a possible explanation, the change in θ_I with neutron number can be related to the band crossing. For nuclei such as ^{164,166}Yb a pronounced backbending is observed, and the feeding time is expected to be shorter than that for the nuclei ^{160,162}Yb due to accelerated feeding transitions in the backbending region according to the band hybridization model. Alternately, this can possibly be due to the effect predicted in ref. [49]. At very high angular momenta, the second minimum in the energy vs. deformation dependence becomes deeper at deformation of about 0.8 than the first minimum at deformation of 0.3. This effect manifests itself more strongly at neutron number $N=88$ and in the vicinity of proton number $Z=66$. This should imply a slower de-excitation for nuclei with N closer to 88 as transitions with changes in the nuclear shape should be retarded.

From a theoretical point of view the side feeding time ϕ_I is a more definite parameter than θ_I. It displays not so strong

increase with decreasing spin (Table 1). However, considerable experimental inaccuracies do not allow one to carry out a detailed quantitative analysis of the dependences $\phi_I(I)$. It is noteworthy that the ϕ_I values are compatible with the experimentally obtained values of the multiplicity of the γ-cascade leading to the population of level I (ref.[26]). It is difficult to make a precise quantitative comparison of the data[26] with our results on the ϕ_I values since the measurements are carried out for reactions induced by ions with strongly different masses: ^{16}O in ref.[26] and ^{40}Ar in the present paper. One may think that the θ_I and ϕ_I values are determined not only by the properties of the high-spin states of a specific isotope, but also by the features of the nuclear reaction leading to the formation of this isotope[28]. In order to clarify the nature of the feeding of high-spin states, one needs a larger amount of experimental data including those on the dependence of θ_I and ϕ_I upon the projectile mass and energy for the same compound nucleus.

We are indebted to Professor G.N.Flerov for his attention to and support of the work. We are also thankful to V.G.Subbotin, N.Djarov, R.Kalpakchieva, L.Alexandrov, S.Iliev, Ts.Venkova, and G.Radonov for their participation at different stages of the work.

REFERENCES

1. A.Johnson, Z.Szymanski. Physics Reports, 7C, 181 (1973); A.Johnson. Extended Seminar on Nuclear Physics, SMR 14/10 (Trieste 1973), Heavy-Ion, High-Spin States and Nuclear Structure (IAEA, Vienna 1975) vol. 1, p. 317.
2. Ø.Saethre, S.A.Hjorth, A.Johnson, S.Jägare, H.Ryde, Z.Szymanski. Nucl.Phys., A207, 486 (1973).
3. R.A.Sorensen. Rev.Mod.Phys., 45, 353 (1973).
4. J.Krumlinde. Nukleonika, 19, 251 (1974).
5. W.Dehnhardt, S.J.Mills, M.Muller-Veggian, U.Neumann, D.Pelte, G.Poggi,B.Povh, P.Taras, Nucl.Phys., A225, 1 (1974).
6. C.Flaum, D.Cline, A.W.Sunyar, O.C.Kistner. Phys.Rev.Lett., 33, 973 (1974).
7. D.Ward, R.L.Graham, J.S.Geiger, H.R.Andrews. Phys.Lett., 44B, 39 (1973); H.R.Andrews, D.Ward, R.L.Graham,J.S.Geiger. Nucl.Phys., A219, 141 (1974).
8. R.M.Lieder, H.Beuscher, W.F.Davidson, A.Neskakis, C.Mayer-Böricke, Y.ElMasri, P.Monseu, J.Steyaert, J.Vervier. Phys. Lett., 49B, 161 (1974).
9. B.Bochev, S.A.Karamian, T.Kutsarova, E.Nadjakov, Ts.Venkova, R,Kalpakchieva. Phys.Scripta, 6, 243 (1973); Preprint JINR, E7-6721, Dubna, 1972.
10. T.K.Alexander, K.W.Allen. Can.J.Phys., 43. 1563 (1965).
11. R.M.Diamond, F.S.Stephens, W.H.Kelly, D.Ward. Phys.Rev.Lett., 22, 546 (1969).
12. B.Bochev, S.A.Karamian, T.Kutsarova, J.Uchrin, E.Nadjakov, Ts.Venkova,R.Kalpakchieva.Yad.Fiz.,16,633(1972);Preprint JINR,P7-6415, Dubna, 1972.

13. B.Bochev, S.A.Karamian, T.Kutsarova, E.Nadjakov, Ts.Venkova, R.Kalpakchieva. Proc.Int.Conf. on Nuclear Physics, Munchen, 1973, vol. 1, p. 298; B.Bochev et al. INDC Consolidated Progress Report, INDC(SEC)-42/L (IAEA, Vienna 1974), p. 45.
14. D.Ward, H.R.Andrews, J.S.Geiger, R.L.Graham, J.F.Sharpey-Schafer. Phys.Rev.Lett., 30, 493 (1973); D.Ward. Proc.Int.Conf. on Reactions Between Complex Nuclei, Nashville (North Holland, Amsterdam 1974), vol 2, p. 417.
15. D.Ward, H.R.Andrews, G.J.Costa, J.S.Geiger, R.L.Graham, P.Taras. Izvestia Akad. Nauk SSSR (ser.fiz.), 39, 37(1975).
16. B.R.Mottelson, J.G.Valatin. Phys.Rev. Lett., 5, 511 (1960).
17. M.Sano, M.Wakai. Progr.Theor.Phys., 47, 880 (1972).
18. F.S.Stephens, R.S.Simon. Nucl.Phys., A183, 257 (1972); F.S.Stephens, P.Kleinheinz, R.K.Sheline, R.S.Simon. Nucl. Phys., A222, 235 (1974); F.S.Stephens. Rev.Mod.Phys., 47, 43 (1975).
19. P.Thieberger. Phys.Lett., 45B, 417(1973).
20. C.K.Ross, Y.Nogami. Nucl.Phys., A211, 145 (1973).
21. B.C.Smith, A.B.Volkov. Phys.Lett., 47B, 193 (1973).
22. J.R.Grover, J.Gilat. Phys.Rev., 157, 802, 814 (1967).
23. J.O.Newton, F.S.Stephens, R.M.Diamond, W.H.Kelly, D.Ward. Nucl.Phys., A141,631 (1970).
24. P.O.Tjøm, F.S.Stephens, R.M.Diamond, J. de Boer, W.E.Meyerhof. Phys.Rev.Lett., 33, 593 (1974).

25. E. der Mateosian, O.C.Kistner, A.W.Sunyar. Phys.Rev.Lett., 33, 596 (1974).
26. G.B.Hagemann, R.Broda, B.Herskind, M.Ishihara, H.Ryde. Proc. Int. Conf. on Reactions Between Complex Nuclei, Nashville (North Holland, Amsterdam, 1974), vol. 1, p. 110; G.B.Hagemann, R.Broda, B.Herskind, M.Ishihara, S.Ogaza, H.Ryde. Nucl.Phys., A245, 166 (1975).
27. J.O.Newton, F.S.Stephens, R.M.Diamond. Nucl.Phys., A210, 19 (1973).
28. B.Bochev, S.A.Karamian, T.Kutsarova, Yu.Ts.Oganessian. Preprint JINR,P7-8676, Dubna, 1975. Yad.Fiz.,23,520(1976).
29. B.Bochev, S.A.Karamian, T.Kutsarova, E.Nadjakov, V.G.Subbotin, J.Uchrin, V.A.Chugreev. C.R.Acad.Bulg.Sci., 25, 905 (1972); Preprint JINR, P6-6229, Dubna, 1972.
30. T.K.Alexander, A.Bell. Nucl.Instr. & Meth., 81, 22 (1970).
31. P.H.Stelson, G.B.Hagemann, D.C.Hensley, R.L.Robinson, L.L.Riedinger, R.O.Sayer. Bull.Am.Phys.Soc., 18, 581 (1973).
32. K.W.Jones, A.Z.Schwarzschild, E.K.Warburton, D.B.Fossan. Phys.Rev., 178, 1773 (1969).
33. J.O.Newton, F.S.Stephens, R.M.Diamond, R.Kotajima, E.Matthias. Nucl.Phys., A95, 357 (1967).
34. B.Bochev, L.Alexandrov, T. Kutsarova. Preprints JINR, P5-7881 and P5-8321, Dubna, 1974.
35. B.Bochev, S.A.Karamian, T.Kutsarova, V.G.Subbotin. Preprint JINR, P7-8033, Dubna, 1974. Yad.Fiz.,22,665(1975).

36. B.Bochev, R.Kalpakchieva, S.A.Karamian, T.Kutsarova, E.Nadjakov, V.G.Subbotin. Preprint JINR, P7-8531, Dubna, 1975.
37. B.Bochev, S.Iliev, R.Kalpakchieva, S.A.Karamian, T.Kutsarova. Preprint JINR, P7-8567, Dubna, 1975.
38. R.M.Diamond, F.S.Stephens, K.Nakai, R.Nordhagen. Phys.Rev., C3, 343 (1971); R.M.Diamond, G.D.Symons, J.L.Quebert, K.H.Maier, J.R.Leigh, F.S.Stephens. Nucl.Phys., A184, 481 (1972).
39. N.Rud, G.T.Ewan, A.Christy, D.Ward, R.L.Graham, J.S.Geiger. Nucl.Phys., A191, 545 (1972); D.Ward, R.L.Graham, J.S.Geiger, N.Rud, A.Christy. Nucl.Phys., A196, 9 (1972).
40. J.Meyer, J.Speth. Yad.Fiz., 17, 1197 (1973); Preprint JINR, E4-6873, Dubna, 1972.
41. D.Karadjov, M.Kirchbach, I.N.Mikhailov, E.Nadjakov, I.Piperova. Proc. Int. Conf. on Nuclear Physics, München, 1973,vol. 1, p. 297; D.Karadjov, I.N.Mikhailov, I.Piperova. Phys.Lett., 46B, 163 (1973); Preprint JINR, P4-8013, Dubna, 1974; Yadern.Fiz., 21, 964 (1975).
42. V.G.Zelevinsky, M.I.Stockman. Proc. of the 24th Conf. on Nuclear Spectroscopy and Nuclear Structure, Kharkov (Nauka, Leningrad 1974), p. 208; M.I.Stockman. Preprint IYF 74-63, Novosibirsk, 1974.
43. D.Karadjov, I.N.Mikhailov, E.Nadjakov, I.Piperova. Preprint JINR, P4-8965, Dubna, 1975.
44. A.Faessler. Proc. Int. Conf. on Reactions Between Complex Nuclei, Nashville (North Holland, Amsterdam, 1974), vol. 2, p. 437.

45. S.G.Nilsson, O.Prior. Mat.Fys.Medd.Dan. Vid.Selsk., 32, no. 16 (1960); O.Prior, E.Boehm, S.G.Nilsson. Nucl.Phys., A110, 257 (1968).
46. Z.Szymanski. Nucl.Phys., 28, 63 (1961); A.Sobiczewski. Nucl.Phys., A93, 501 (1967).
47. K.Kumar. Phys.Rev.Lett., 30, 1227(1973).
48. A.Molinari, T.Regge. Phys.Lett., 41B, 93 (1972); R.A.Broglia, A.Molinari,G.Pollarolo, T.Regge. Phys.Lett., 50B, 295 (1974); 57B, 113 (1975).
49. K.Neergard, V.V.Pashkevich. Preprint JINR, P4-8947, Dubna, 1975;

Received by Publishing Department
on March 22, 1976.